(4)

MEMORANDUM REPORT BRL-MR-3740

BRL

SMALL SCALE TESTING OF A MASS-STABILIZED ELECTROMAGNETIC PROJECTILE

JAMES M. GARNER
ALEXANDER E. ZIELINSKI

MARCH 1989

U.S. ARMY LABORATORY COMMAND

BALLISTIC RESEARCH LABORATORY
ABERDEEN PROVING GROUND, MARYLAND

DESTRUCTION NOTICE

Destroy this report when it is no longer needed. DO NOT return it to the originator.

Additional copies of this report may be obtained from the National Technical Information Service, U.S. Department of Commerce, Springfield, VA 22161.

The findings of this report are not to be construed as an official Department of the Army position, unless so designated by other authorized documents.

The use of trade names or manufacturers' names in this report does not constitute indorsement of any commercial product.

UNCLASSIFIED
SECURITY CLASSIFICATION OF THIS PAGE

REPORT DOCUMENTATION PAGE

Form Approved
OMB No. 0704-0188

1a. REPORT SECURITY CLASSIFICATION UNCLASSIFIED	1b. RESTRICTIVE MARKINGS
2a. SECURITY CLASSIFICATION AUTHORITY	3. DISTRIBUTION / AVAILABILITY OF REPORT Approved for public release; distribution is unlimited.
2b. DECLASSIFICATION / DOWNGRADING SCHEDULE	
4. PERFORMING ORGANIZATION REPORT NUMBER(S) BRL-MR-3740	5. MONITORING ORGANIZATION REPORT NUMBER(S)
6a. NAME OF PERFORMING ORGANIZATION U.S. Army Ballistic Research Laboratory 6b. OFFICE SYMBOL (If applicable) SLCBR-LF	7a. NAME OF MONITORING ORGANIZATION
6c. ADDRESS (City, State, and ZIP Code) Aberdeen Proving Ground, MD 21005-5066	7b. ADDRESS (City, State, and ZIP Code)
8a. NAME OF FUNDING / SPONSORING ORGANIZATION U.S. Army Ballistic Research Laboratory 8b. OFFICE SYMBOL (If applicable) SLCBR-DD-T	9. PROCUREMENT INSTRUMENT IDENTIFICATION NUMBER
8c. ADDRESS (City, State, and ZIP Code) Aberdeen Proving Ground, MD 21005-5066	10. SOURCE OF FUNDING NUMBERS PROGRAM ELEMENT NO. 62618A; PROJECT NO. 1L1 62618AH80; TASK NO.; WORK UNIT ACCESSION NO.

11. TITLE (Include Security Classification)
Small Scale Testing of a Mass-Stabilized Electromagnetic Projectile (U)

12. PERSONAL AUTHOR(S)
Garner, James M., and Zielinski, Alexander E.

13a. TYPE OF REPORT	13b. TIME COVERED	14. DATE OF REPORT (Year, Month, Day)	15. PAGE COUNT
Memorandum Report	FROM _____ TO _____	January 1989	26

16. SUPPLEMENTARY NOTATION

17. COSATI CODES			18. SUBJECT TERMS (Continue on reverse if necessary and identify by block number)
FIELD	GROUP	SUB-GROUP	Mass-Stabilized Electromagnetic Projectile Testing Electromagnetic Launch
01	01		

19. ABSTRACT (Continue on reverse if necessary and identify by block number)

Few electromagnetic (EM) gun projectiles that incorporate aerodynamic aspects have been fired from an EM gun. A practical EM gun projectile, to be used in atmospheric conditions, should consider how efficiently the projectile package is accelerated as well as the flight characteristics. This report details the firing of a full-bore projectile from an electromagnetic gun. Background projectile design criteria, test procedures, and results are discussed.

20. DISTRIBUTION / AVAILABILITY OF ABSTRACT ☐ UNCLASSIFIED/UNLIMITED ☒ SAME AS RPT. ☐ DTIC USERS	21. ABSTRACT SECURITY CLASSIFICATION UNCLASSIFIED
22a. NAME OF RESPONSIBLE INDIVIDUAL James M. Garner	22b. TELEPHONE (Include Area Code) (301)-278-4680 22c. OFFICE SYMBOL SLCBR-LF-A

DD Form 1473, JUN 86 Previous editions are obsolete.

SECURITY CLASSIFICATION OF THIS PAGE
UNCLASSIFIED

Acknowledgements

This work is supported by the Close Combat Armament Center, ARDEC, Dover N.J. through the Joint Services Small Arms Program. The technical assistance of Dr. Keith A. Jamison is greatly appreciated.

Table of Contents

List of Figures

I. INTRODUCTION

Research addressing the utilization of electromagnetic (EM) launchers in a weapons role has been in existence for some years.[1,2,3] In particular, the parallel rail launcher configuration has been focused on extensively. A large percentage of work has been devoted to acceleration and electrical performance rather than on the package to be accelerated. In this test, more attention was given to the launch package, in part, because its lethality is the ultimate measure of effectiveness of an EM launcher. The design of the launch package is complicated by the numerous tasks it must perform. A portion of the total launch package must serve as the armature in the electric gun. The armature must withstand the magnetic forces and serve as the accelerator of the package. For atmospheric flight, part of the launch package must serve as an aerodynamic body, flying the payload to the target. Finally, some portion of the launch package must perform the task of defeating the target.

In order to assess the practicality of a small-caliber EM launcher, the designer must consider the projected improvements offered over existing weapons technology. The .50 caliber Saboted Light Armor Penetrator (SLAP) round represents the existing technology and was used for comparison. Bore sizes of less than 15.25 mm (.60 in) were considered small-caliber.

The EM projectile is shown in Figure 1, and it is essentially a scaled down version of a previous design.[4] The projectile has a square base of 10 mm (.400 in), and this was considered the projectile's reference length (.400 in =1 caliber) for all measurements. The projectile's tungsten nose section is 2.5 calibers long. This choice of nose length results in a weight distribution of 35% to 65% nose to afterbody. A threaded tungsten stud joined the nose and afterbody. A slot 3.4 mm (.133 in) wide and 14.3 mm (.563 in) deep is shown at the rear of the projectile. The thickness of the leg cross sections on either side of the slot is 3.4 mm. A plastic bore rider supports the tungsten/aluminum joint and was 1.25 calibers in length.

The objective of the test program was to examine rail/projectile interaction, projectile launch and general flight characteristics. A short description of an EM launcher is included in Appendix A.

II. SET-UP AND PROCEDURE

A sketch of the experimental set-up is shown in Figure 2. It consisted of a 300 kJ capacitor bank coupled to a pulse shaping inductor. These devices store and regulate the power for a one-meter-long, nominally 10 mm square bore rail gun. More elaborate and efficient rail gun systems exist, [5,6] but the test was constrained to use the system at Maxwell Laboratories. An injector is attached at the breech of the rail gun and drives the projectile using high pressure gas. An injection velocity is necessary to prevent spot welding that sometimes occurs with solid armatures that start from rest. Injection increases the potential for higher velocity without the increased frictional and ohmic dissipation to the armature contact surfaces that are common at lower starting velocities.

The X-ray film, located approximately 15.2 cm (6.0 in) from the exit of the gun, was used to examine the level of yaw at the muzzle exit. Following the X-ray film, five yaw cards were spaced equally from 2.28 to 4.42 m (7.5 to 14.5 ft) from the gun exit. These cards were positioned for analysis of the predicted yawing motion of the round. Beyond the yaw cards, break-wires measured the projectile velocity near the target. The target was a one-inch-thick piece of rolled homogeneous armor (RHA) enclosed in a 46.2 cm (18.9 in) square steel catcher box positioned 8.84 m (29.0 ft) from the muzzle. A video camera was positioned 4.27 m (14.0 ft) from the gun exit to obtain an in-flight photograph of the projectile. The video camera did not provide adequate resolution and was eventually replaced for the last two rounds of the test with a high speed framing camera at the same location.

Instrumentation of the gun was a major aspect of the test. Two pressure gages located in the injector section detected the projectile's longitudinal position. A pair of insulated high voltage contacts, 'hot rail contacts', were located in the injector section and provided a trigger signal marking the projectile arrival time and position. Voltages and currents pertinent to the operation of the railgun and projectile were recorded digitally. The primary electrical measurement evaluating the performance of the projectile is the voltage measured across the rails at the muzzle, which is the armature voltage. An alternate voltage measured at the breech could also be used. This measurement, however, contains additional voltage contributions due to a moving conductor in a magnetic field (back EMF) and rail resistance. Both the breech and muzzle voltages were measured by resistively dividing a portion of the main driving current and measuring that small current with a current transformer. The armature current is the sum of two currents and each was measured by a Rogowski coil. Inside the railgun, magnetic field probes were oriented to sense the time rate of change of the armature and rail magnetic field as the projectile passes by. These probes, commonly called B dot probes, give the position of the centerline of current flow in the armature. Four holes were bored in the insulator section of the gun to accommodate the magnetic field probes and each also served as a position marker.

The test program included firing eleven projectiles. The first three firings checked the injector system only and are called gas shots. The data gained from these shots helped determine a velocity versus gas pressure relationship. The next projectiles were fired at low current levels, close to 125 kA, with injection velocities of about 300 m/s. These firings examined armature effectiveness at lower current levels with minimum risk of rail damage. Higher current increases the probability of arcing and concurrent rail damage. For the test program, a lack of projectile structural integrity, high voltage arcing, and severe armature damage prior to impact were considered critical failures.

III. RESULTS

Table 1 is a shot summary and contains in-bore velocities, injection velocities, current levels, break-wire velocities, armature conditions and comments.

Table 1. Shot Summary

Shot #	In-bore Velocity (m/s)	Injection Velocity (m/s)	Peak Current (kA)	Break-wire Velocity (m/s)	Armature Condition	Comments
1	—	No data	Gas shot	No data	Gas shot	Broken nose
2	—	174.3	Gas shot	249.8	Gas shot	Broken nose
3	—	333.3	Gas shot	406.7	Gas shot	Broken nose
4	No Data	339.3	130	500.0	Minor damage	Broken nose
5	568	333.3	132	No Data	Minor damage	Flew intact
6	571	333.3	131	510.2	Minor damage	Flew intact
7	—	No data	Gas shot	No data	Gas shot	Broken nose
8	—	No data	Gas shot	No data	Gas shot	Broken nose
9	624	365.4	127	No Data	Minor damage	Unbroken screw
10	582.7	333.3	131	367.6	Minor damage	Broken nose
11	1070.6	380	270	No Data	Severe damage	No flight data

1. GAS SHOTS

Testing started with three gas shots. These shots verified the functioning of the injector and the hot rail contact, and they determined a time delay for capacitor bank discharge. For these shots the gas pressure was varied from 12.4 MPa (1800 psi) to 23.4 MPa (3400 psi). The resultant velocities at these pressures are shown in Table 1. The yaw card data indicated that the noses had broken away from the afterbodies. The bore rider was apparently blown in front of the projectile by high-pressure gas that leaked forward around the base of the projectile. Consequently the projectile traveled with its nose section unsupported down the bore. Without support, balloting of the projectile probably fractured the nose while in-bore. Despite the probable reoccurrence of the bore rider being blown off, it was thought that important armature data could be obtained. No X-ray data were obtained for these shots.

2. ELECTRICAL SHOTS

a. Shot 4

The capacitor bank was charged to 3000 volts, and the accumulator pressure remained at roughly 23.4 MPa (3400 psi). The projectile was injected at 339 m/s and accelerated by a peak current of 130 kA. The initial charge voltage was essentially kept constant for the remaining shots. The velocity measured at the break wires showed a 23% increase over gas shot velocities. The muzzle voltage trace showed a large spike as the projectile exited indicating that current was still flowing in the gun circuit at that time. The projectile nose broke as expected.

b. Shot 5

For this shot, the bore rider split axisymmetrically. The projectile remained intact throughout the flight according to yaw card data. The yaw decreased during the flight, going from roughly 17 degrees to under 10 degrees over a distance of 2.14 m (7.02 ft). This corresponded to a yaw period of approximately 13.7 m (45 ft). Predictions of this period were within 10% of this measurement.

c. Shot 6

Modifications were made for Shot 6 to fix the position of the bore rider on the projectile during acceleration. The bore rider was cut to aid in axisymmetric discard, and epoxied to the exterior threads at the nose/afterbody joint (these threads are hidden by the sabot in Figure 1). In addition, the slot in the afterbody was filled with epoxy in an attempt to stop high pressure gas from leaking forward through the projectile slot. The bore rider's corners were rounded to allow gas leaking up from the rear to flow past the bore rider, thereby helping to keep the bore rider on the projectile until exit. The first successful X-rays of the test showed the bore rider discarded just out of the gun. Unfortunately, the discard was asymmetric. Figure 3 shows the round after impact.

The projectile appears to have flown intact to the target according to yaw card data. The yaw of the projectile stayed roughly at the same level varying from 9 degrees to 11.5 degrees in approximately 2.14 m. The yaw data for this round indicated a period of 18.5 m (60 ft). Most of the armature damage for this round occurred on impact, however, some surface pitting can be seen over much of the legs. X-ray data revealed a concave shaped lower leg upon projectile exit. Pressure from in-bore arcing at the rail contact interface is thought to have caused this concavity. The extent of the arc damage on this shot does not appear serious enough to have a marked effect on the projectile flight characteristics.

d. Shots 7 and 8

These shots suffered hot rail electrical contact problems and the capacitor bank did not discharge. On Shot 8 the nose fractured at the tungsten/aluminum (W/Al) interface despite previous bore rider and projectile modifications.

e. Shot 9

The tungsten nose was replaced with a steel screw to examine if the steel screw would fracture as readily as the tungsten nose. The steel screw did not fracture. The X-ray photographs at the projectile exit revealed the head of the steel screw preventing the bore rider from fully advancing off the aluminum afterbody. This proved that gas pressure was forcing the bore rider ahead of the projectile leaving the nose unsupported. Due to the weight reduction in using a steel screw instead of a tungsten nose, the injection velocity was boosted to 365 m/s. The projectile legs showed definite signs that an arc formed.

f. Shot 10

The projectile used for Shot 10 had an armature contact surface with serrations to increase the current carrying capability. Multiple points of contact, which occur when an armature contact surface is serrated, help prevent in-bore arcing. Figure 4, showing Shot 10 after impact, shows the serrations. There were six, .508 mm (.020 in) wide cuts spaced 1.02 mm (.040 in) apart and to a depth of 1.02 mm. The cuts were perpendicular to the axial direction and canted rearward at a 45 degree angle. In addition, the inside corners of the legs were tapered at a 15 degree angle to improve the current density and uniformly distribute the magnetic contact force. X-ray photographs showed a slightly bent nose still attached to the afterbody upon projectile exit, but the framing camera showed a highly yawed projectile without a nose section.

g. Shot 11

The current level was doubled for this shot. The projectile for this shot had about half the number of serrations on the contact surface compared to the previous shot. This shot showed a total loss of projectile/armature structural integrity and indicated that the armature was inadequate for these current levels.

3. SHOT DISCUSSION

a. Electrical Considerations

The gas pressure yielded injection velocities near 330 m/s, which were adequate to prevent spot welding. The muzzle and breech voltage were adequately recorded for one shot (Shot 4). A plot of the armature current, and breech and muzzle voltages are shown in Figures 5 and 6. A convenient technique to evaluate the Joule heating of a conductor is by the use of the action integral. The action integral is simply the integral of the current squared over time divided by the cross sectional area squared. Since the current enters at the rear of the leg, the cross section is the leg thickness times the bore height. This is set equal to the action constant, which implicitly gives the temperature rise of the conductor. The action constant has been tabulated for a variety of conductors.[7] The integral of the current squared is evaluated up to the time when the armature transitions to an established arc. Solid aluminum armatures with flat contacting surfaces have arced, regardless of velocity, at action constants of 8×10^{15} $amps^2 \cdot s/m^4$. This translates to a bulk temperature rise of only 140° C. This value was also obtained from tests performed on the .50 caliber mass-stabilized projectile with a leg thickness of 2.54 mm (.10 in). In more recent testing at the Ballistics Research Laboratory, a 6.35 mm (.25 in) mass-stabilized design has been operated at 8×10^{15} $amps^2 \cdot s/m^4$ with no arcing. However, modifications were made to the contact surface area to increase the current carrying capability. The point of transition is marked by a rise in voltage to a level indicative of armature failure. This level is bore size dependent, and for the 10 mm barrel it is 100 volts. Single contact arcing, without emitting light, occurs in the 10 - 20 volt range. Light is emitted for a single

contact arcing at 40 - 60 volts. Visual inspection of the rails after a shot should show the exact axial position and rail location of contact arcing. The muzzle voltage record for Shot 4, (see Figure 6), revealed the armature contacting intermittently, breaking from the rail with greater frequency until an arc was fully established at 620 μs. This arc voltage continues at the 100 volt level until the projectile exits the barrel at 1.7 ms. The action integral constant calculated from the current trace up to 620 μs is 5×10^{15} amps^2·s/m^4; this corresponds to a bulk temperature rise, due to ohmic heating, of only 87°C. This is consistent with previous data.

Dimensional tolerances play a crucial role in the function of the armature. If the projectile rapidly enters a region where the dimension of the leading edge of the contact surface is less than that of the armature contact surface, the legs become overstressed causing the trailing edge of the legs to lift away from the rail. This leg movement would likely cause an arc to form. This arc would cause high pressures and further leg bending. The straightness of the barrel is also important since off-axis components of high acceleration cause side loads that damage parts of the projectile. The bore used was honed and shimmed to obtain the overall dimensions required for the armature before it was considered usable. Tighter bore tolerances were attempted in order to improve projectile launch conditions. Because of the lack of electrical data on the armature, it is difficult to analyze the armature function and the position in the barrel where the arc formed. However, based on experience from firing a projectile at lower energy, it is possible to determine whether an arc formed. On full-scale testing of a 12.7 mm diameter projectile at BRL, when an arc occurred, there was a notable increase in final velocity. Numerical simulations were performed using the actual gun current profile and predicted a much lower velocity for nonarcing firings. The plasma pressure, resulting from the formation of an arc, contributes a driving force not accounted for in the simulation. For the 10 mm shots, assuming a perfect armature, the simulation predicts muzzle velocities of 425 m/s. This is substantially lower than any of the exit velocities measured. Hence, it is believed that all of the armatures arced in-bore. Arcs from solid armatures can cause much in-bore damage and rail erosion and are, therefore, to be avoided. The X-ray photograph of Shot 6, revealed that the upper armature leg is concave upon gun exit. This is likely the result of the legs lifting off the rail surface and an arc striking in the resulting gap.

b. Mechanical Considerations

An effective EM projectile must maintain structural integrity and be aerodynamically efficient. Given these characteristics and the fact that future EM projectiles may be based on early designs such as this, it is critical that the fracture and separation of the nose section be understood. During the projectile's travel down the bore, side loads can occur due to bore asymmetries. An analysis was performed to compute the bending moment necessary to break the nose at the threaded section of the stud. Calculation, assuming pure bending, revealed that a bending moment of 1.01 N·m (8.96 lb·in), at the minor diameter, could cause a break. A load of 120 N (27 lbs) exerted at the center of gravity of the nose section would result in a moment of this size. Additional stresses contribute to the fracture of the tungsten stud. A section view, without external threads, is shown in Figure 7. A failure in the shear mode was calculated to occur for a load of 1000 N (225 lbs)

at the minor diameter. The exact combination of bending and shear effects that actually occur is unknown. A change to a thicker tungsten stud could resist these forces and keep the mass properties of the projectile nearly the same.

Two tests using a static load machine were performed to get a more accurate measure of the forces required to break the nose section. The projectile armature contact surfaces were rigidly supported, and the test configuration resembled a cantilevered beam with the nose section and a portion of the afterbody unsupported as can be seen in Figure 8. Loads of 488 N (110 lbs) and 400 N (90 lbs) caused the nose to break just prior to the threads at a radius located 2.83 cm (1.11 in) from the support point. These loads, while static and not dynamic in their application, represent a significant fraction (approximately 10%) of the accelerating force.

Several theories have been suggested for the failure of the nose section. An asymmetric bore coupled with high accelerations can cause large side loadings on the nose. Another hypothesis was that the acceleration load caused the projectile to fail in compression. An examination of the stresses using the Algor Supersap stress analysis code indicates otherwise.[8] Using a current of 130 kA, the corresponding acceleration was 31,000 g's. The highest stresses occur at the radius prior to the threaded section in Figure 9. This radius has essentially the same diameter as the minor diameter of the threads. The greatest compressive stress resulting from this inertial loading was well below the yield strength of the tungsten nose. The nose/afterbody joint from the acceleration standpoint is adequate.

All nose/afterbody fractures were assumed to have happened in-bore. Data from yaw cards clearly show that some noses have separated from the afterbodies 2.13 - 3.05 m (roughly 7 to 10 feet) from the gun muzzle. In contrast to this, X-ray photographs at .152 m revealed that some projectiles appeared to have remained intact. An explanation reconciling the conflicting data is that the fracture happens in-bore but the nose has not yet been able to separate from the projectile at the time of the X-ray picture. Upon completion of the testing, the rails were examined for signs of in-bore scoring, which might occur with a fractured nose that separated in-bore , and none were found. The point along the travel where the projectile nose broke remains undetermined.

4. COMMENTS

The physical, photographic, and electrical data gathered were inconsistent and afforded only glimpses of what happened on individual shots. Current traces were obtained and were useful in calculating the maximum acceleration of the projectile. Primary armature data, such as the voltage drop across the rails at the muzzle and at the breech were recorded, but acceptable data were obtained only for Shot 4. The surface of most of the armatures showed that melting was taking place along the entire rail/armature interface. Figure 10 shows an example of contact surface melting from Shot 4. Electrical heating of the resultant plasma arc when the armature leg loses rail contact is sufficient to cause this extensive melting. It is believed that excessive loading at the front of the armature slot, as occurs in an undersized bore, caused the armature legs to fail.

In general, the rails suffered only surface damage during the eleven shots. There were dark areas on the inner rail surfaces where arcing or a melting of aluminum appeared to have occured. The rails were not examined after every shot due to the difficulty involved with assembling and disassembling the gun. Therefore, it is not known which shots caused the most damage. Visual examination of the rails showed a thin aluminum coating in sections confirming that armature melting did occur although the exact reason is not known.

IV. CONCLUSIONS

Projectiles that are equivalent aerodynamically and structurally, have been launched under the same acceleration conditions at BRL. [9] These projectiles exhibited none of the mechanical problems that occurred during the testing at Maxwell. Small modifications were made to these rounds though. These modifications included increasing the number of serrations on the contact surface, chamferring interior slot edges and lengthening the bore-rider to 1.9 calibers. The launcher used at BRL did not create excessive leg loadings that would cause the armature legs to lose contact and fail. From this, it is believed that the gun integrity is a major factor in successful railgun firings.

Improvements to the projectile design and some railgun requirements came about as a result of this testing. With regard to the railgun itself, the rail to rail dimensions were shown to be very important to the proper functioning of a projectile. Knowing the expansion of the bore under pulsed current conditions can assist in calculating the armature interference fit and help to minimize frictional losses. The projectile's tungsten/aluminum interface should be modified by enlarging the diameter of the threaded tungsten stud for greater strength. This will enable the projectile to survive larger than expected side loads. The armature configuration showed promise, and in general worked adequately at the low current levels despite some in-bore arcing. Thicker armature legs and armature surface serrations will undoubtedly increase the current carrying capability and allow higher speeds.

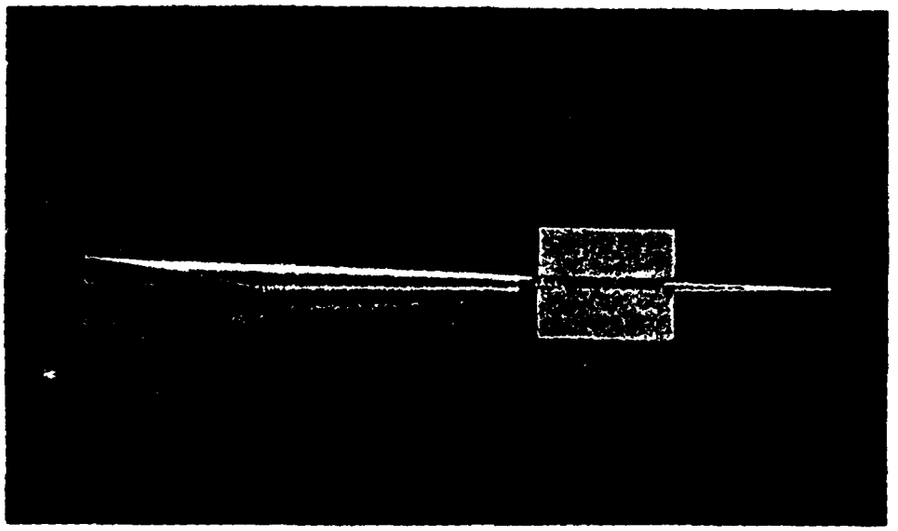

Figure 1. 10 mm test projectile.

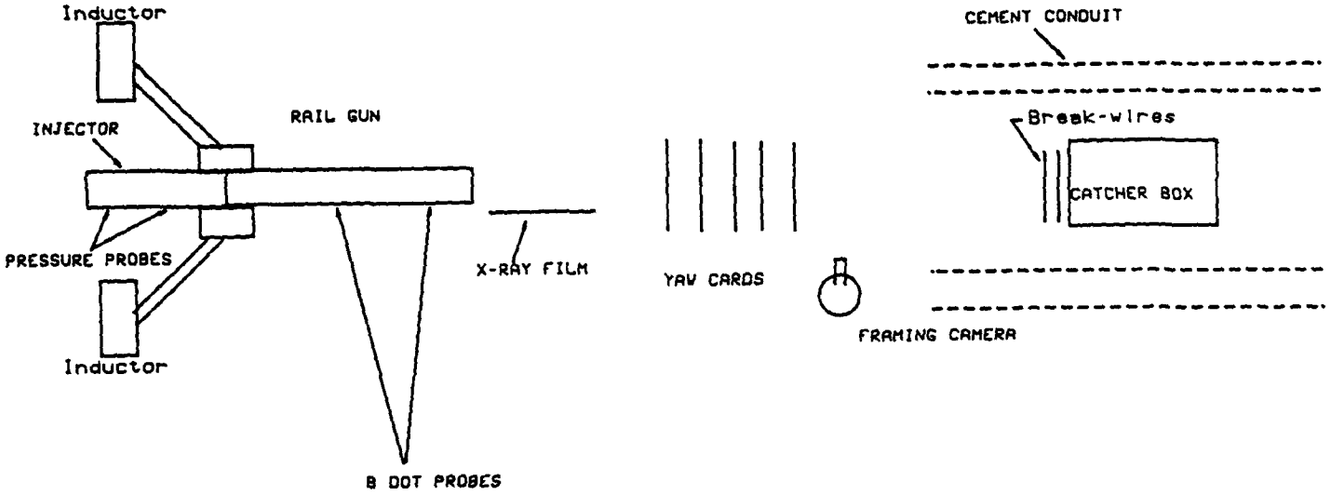

Figure 2. Experiment layout.

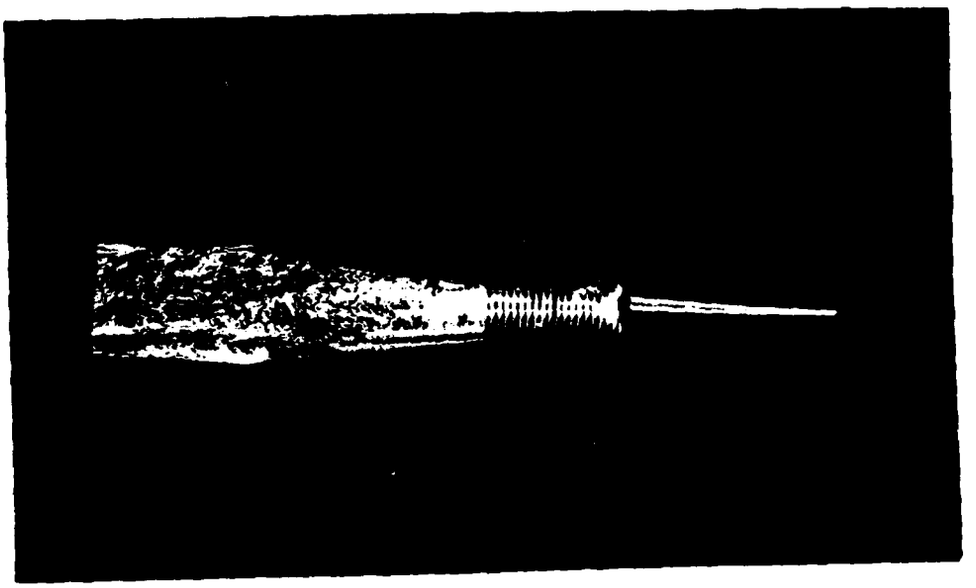

Figure 3. Projectile after impact (Shot 6).

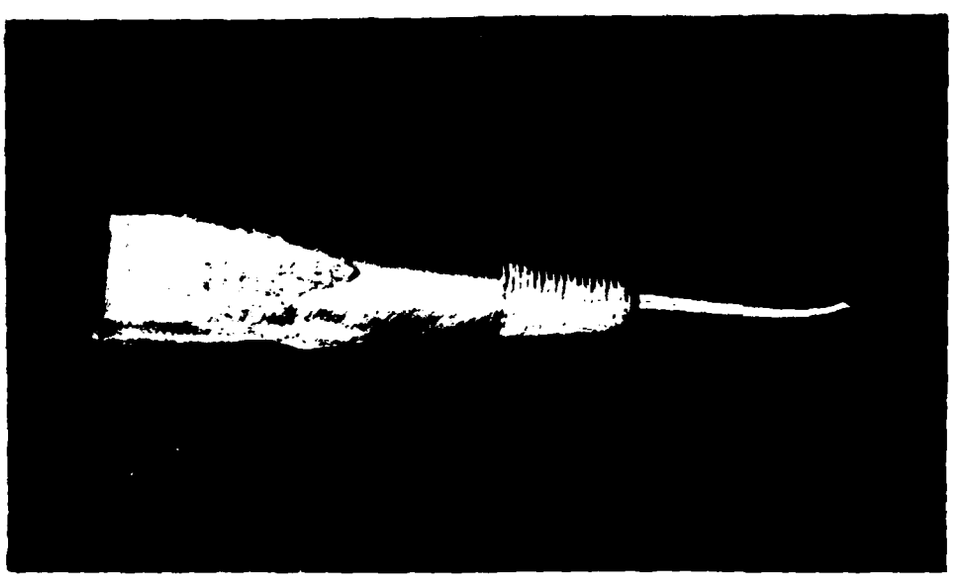

Figure 4. Recovered projectile (Shot 10) showing visible serrations.

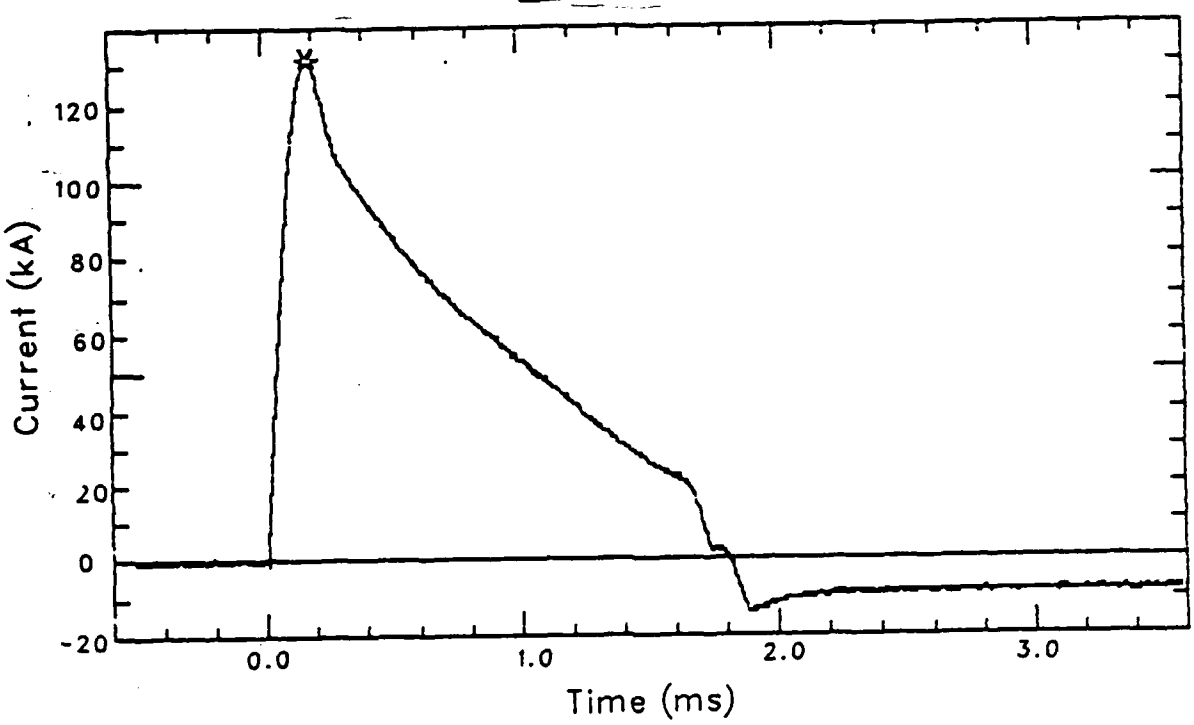

Figure 5. Current vs. time (Shot 4).

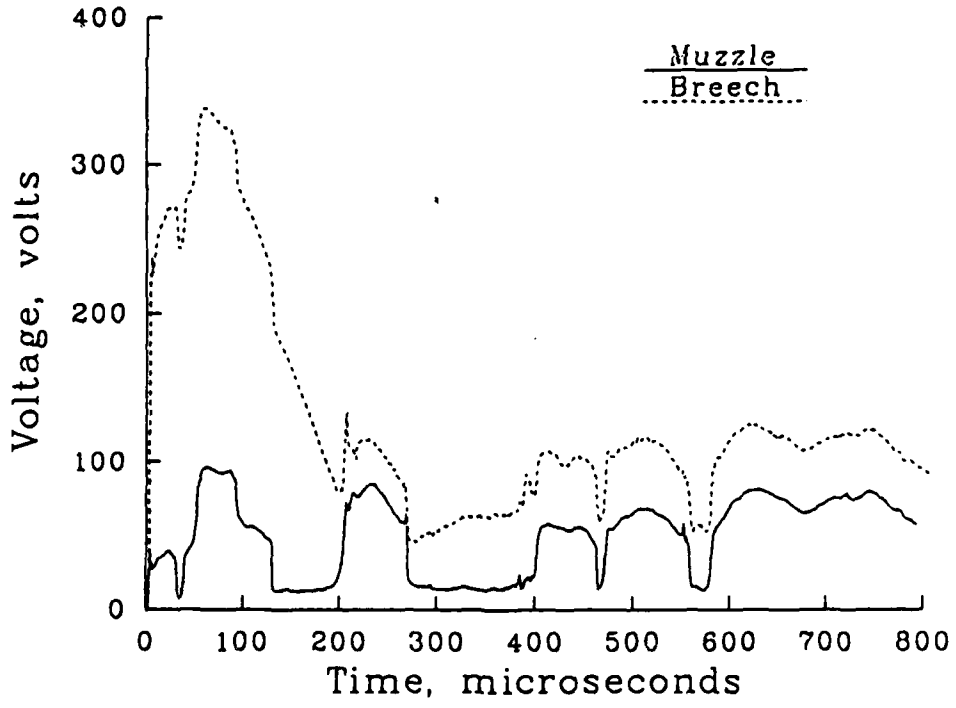

Figure 6. Breech and muzzle voltage vs time (Shot 4).

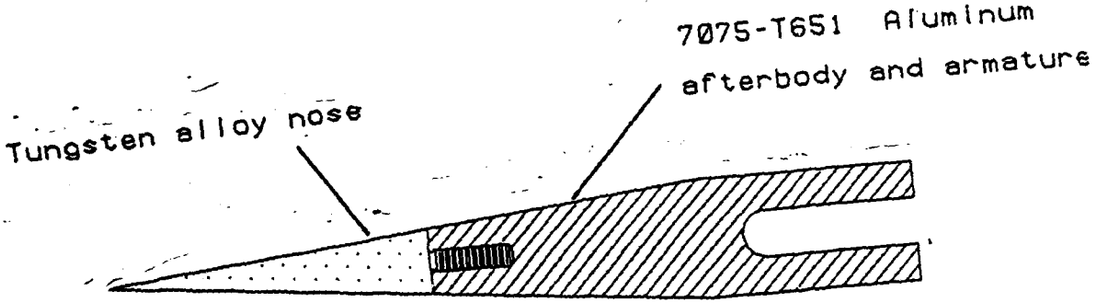

Figure 7. Section view of the projectile

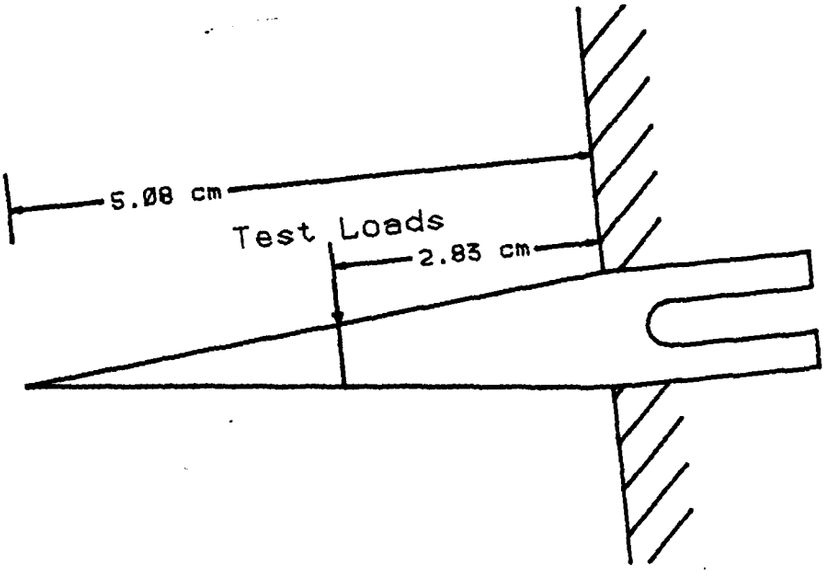

Figure 8. Test loading on the projectile

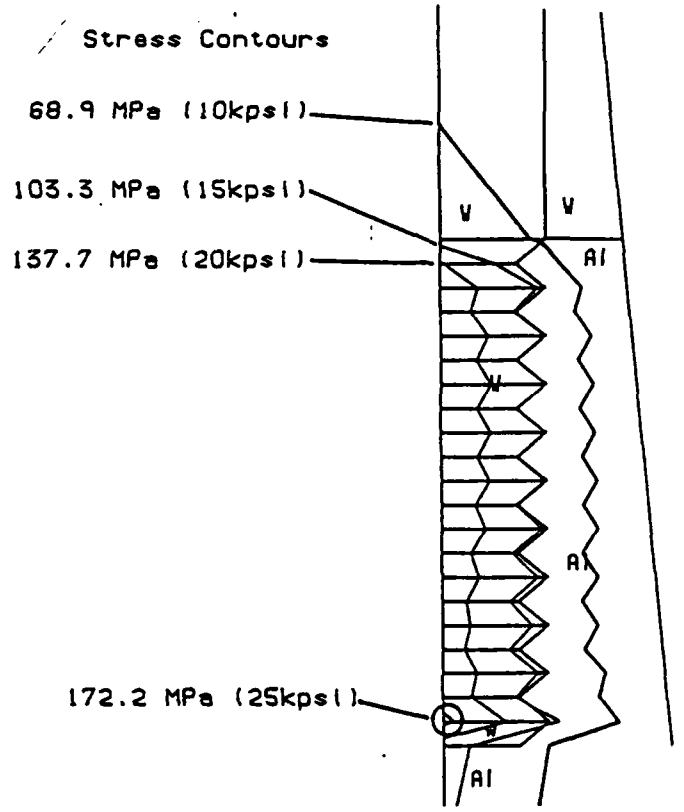

Figure 9. Predicted stresses for 10 mm model for a 31,000 g load.

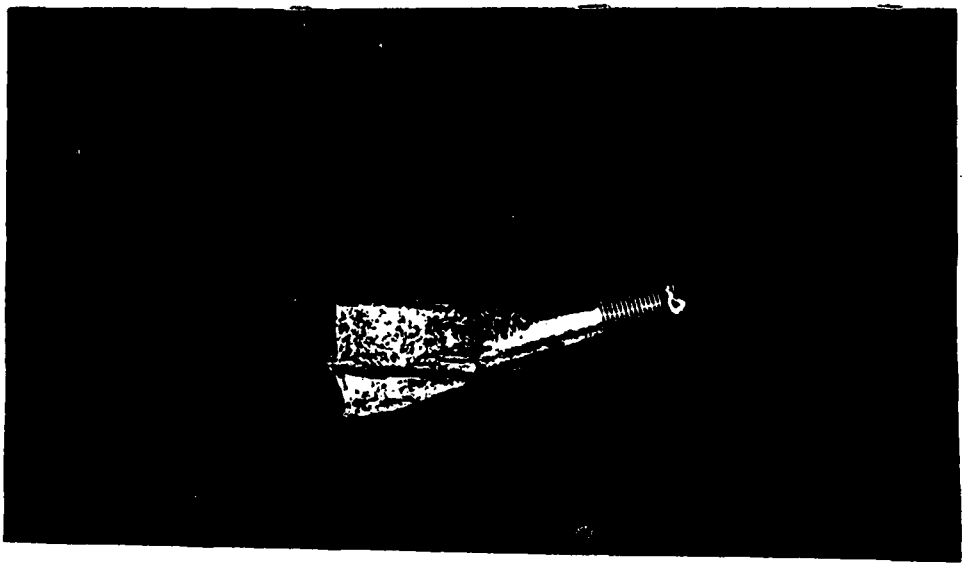

Figure 10. Surface contact melting.

References

1. Barber, J.P., McCormick, T.J., and Bauer, D.P.,"Electromagnetic Gun Study," AFATL-TR-81-82, September 1981.

2. Bechtol, T.R., - Ed., May, I., Temperly, J., Johnson, L., and Mester, J.,"An Assesment of Gun Propulsion Technologies at the Ballistic Research Laboratory and Their Weapons Systems Potential (U)," ARBRL-SP-00024, January 1983, (Confidential).

3. Gavert, R. P., "Lethality Testing Involving Railgun Structures," IEEE Transactions on Magnetics, Vol 22, Number 6, Nov. 1986.

4. Garner, J., Zielinski, A., and Jamison, K.A.,"Design and Testing of a Mass Stabilized Projectile for a Small Caliber Electromagnetic Launcher," Presented at the 4th IEEE Symposium on Eletromagnetic Launch Technology, Austin TX, 1988.

5. Pratrap, S.B., Driga, M.D., Weldon, W.F., and Spann, M.L., "Future Trends For Compulsators Driving Railguns," IEEE Transactions on Magnetics, Vol. 22, Number 6, Nov. 1986.

6. Zielinski, A., and Jamison, K.A.,"A Solid State Switched Power Supply For Simultaneous Capacitor Recharge and Railgun Operation," Presented at the 4th IEEE Symposium on Electromagnetic Launch Technology Austin Texas, April 1988.

7. Tucker, T.J., and Toth, R.P., "EBW1: A Computer Code for the Prediction of the Behavior of Electrical Circuits Containing Exploding Wire Elements," SAND-75-0041, Sandia Laboratories, April 1975.

8. "Algor Supersap" Algor Interactive Systems Inc, Pittsburgh, Pa. 15206.

9. Zielinski, A.," BRL PULSED POWER LABORATORIES FACILITIES" Proceedings from 5th Electromagnetic Launcher Association Meeting, Sept 1988, Auburn, AL.

APPENDIX A

BACKGROUND

Railgun launch packages are mainly comprised of two parts: an armature section and a payload section. While extensive efforts are being given to developing an efficient armature, much less attention is being given to integrating the armature with the payload. Launch package designs with discarding armatures pay a significant kinetic energy penalty between launch and flight. From an energy standpoint, a flight body with an integral armature is efficient. For small caliber applications, combining the armature and payload masses is very attractive. Although the idea is simple, the details of this integration between armature and payload are complex.

The rearward section of the afterbody conducts the current from rail to rail, and it is referred to as the armature. The base of the afterbody is slotted and has two extensions. These extensions are termed legs. The flat surfaces of the legs that touch the rails are referred to as armature contact surfaces. The armature legs have a tapered interference fit between the rails and the armature contact surface to establish an initial pre-load on the surface. This maintains current flow through the interface before the projectile has started to accelerate. The resultant Lorentz force, due to current flow in a magnetic field, drives the projectile forward and tends to expand the slot and further increases the contact pressure on the armature contact surfaces.

A diagram of an electromagnetic railgun is shown in figure A-1. The railgun, in its simplest form, operates by applying current to a stationary parallel pair of conducting rails. A conductor, either solid or gaseous, is free to slide between the rail pair. This moving, conducting element is called the armature and carries the current to the opposite rail. The interaction between the current and its magnetic field produces a force proportional to the square of the current. This force accelerates the armature. The highest performance case is for constant acceleration and likewise constant current. However, for most efficient operation the current must go to zero upon projectile exit. Ideally the driving current waveform should be a square wave. Unfortunately a true square wave is not a practical possibility. Continued research in pulsed power rotating machinery[5] and capacitor and switching technology[6] is being pursued to further refine acceleration profiles. These choices of pulsed power can attain near sinusoidal current pulses with half cycle times that can be matched to the acceleration time of a projectile in the bore. Nonetheless, an easy and typical technique to obtain nearly constant acceleration (at the expense of lower efficiency) is to create a current pulse, I, which decays slowly compared to the acceleration time. This requirement is satisfied by the power supply circuit shown in figure A-2. Primed letters denote quantities associated with the railgun part of the circuit. Resistive, capacitative, inductive quantities are noted by R's, C's and L's with varying subscripts. Further explanation of these quantities and their purpose is given in Reference 6.

The circuit works as follows. The capacitor, in figure A-2, is charged to a desired voltage. When the discharge is initiated (S1 closes) the resulting sinusoidal current waveform charges the inductor to maximum energy in a time short compared to the acceleration time. A second switch (S2) is then closed across

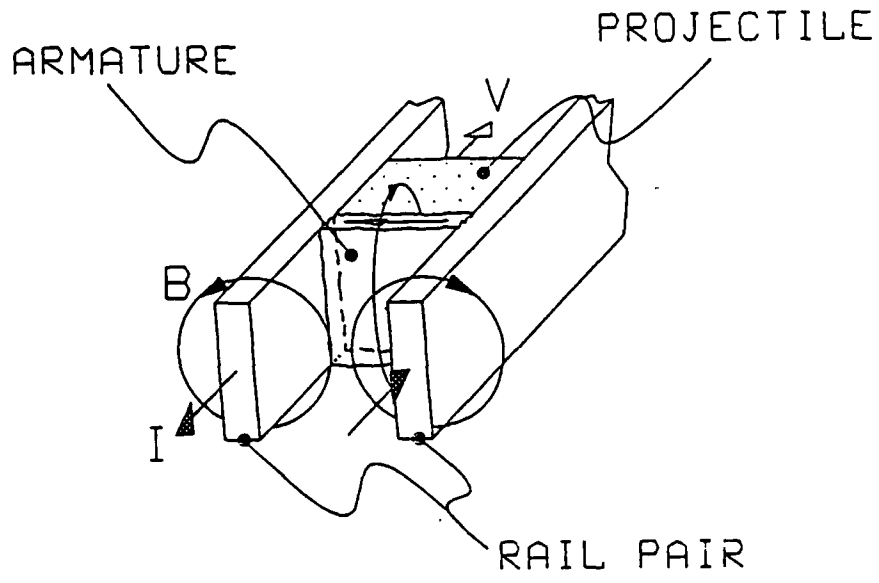

Figure A-1 Diagram of Electromagnetic Railgun

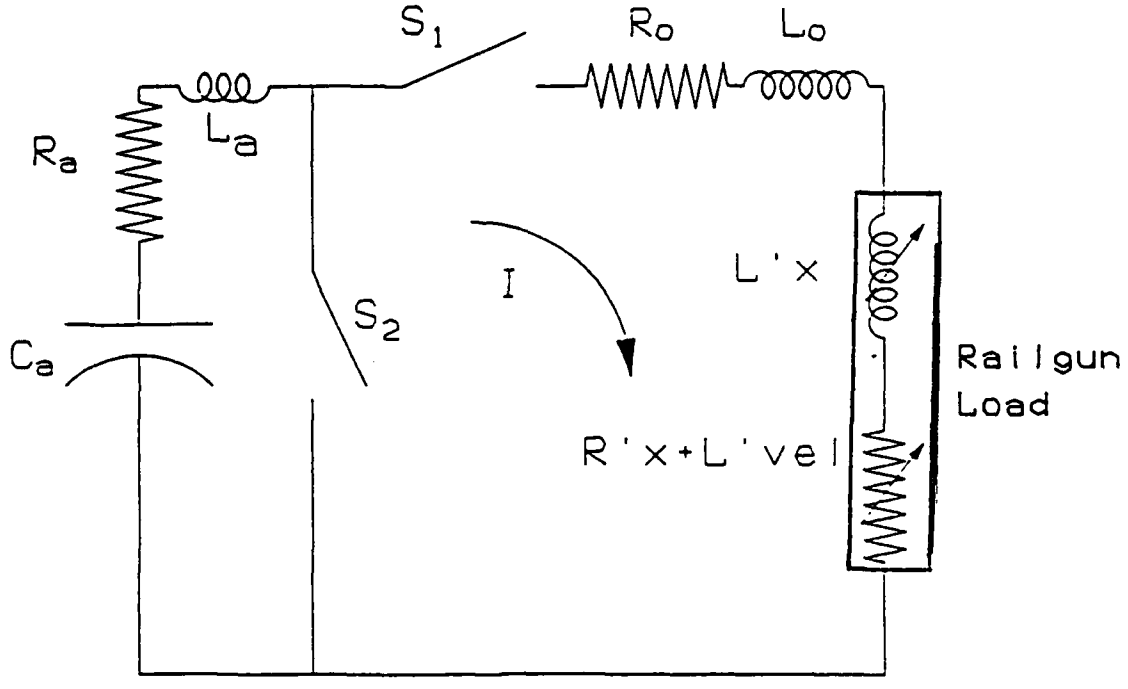

Figure A-2 Railgun Power Supply Circuit

the capacitor to prevent voltage reversal and to create an exponentially decaying current waveform. In addition to this circuit's inefficiencies, there will still be current flowing in the circuit when the projectile exits the gun barrel. When this inductive circuit is opened, the resultant magnetic fields try to collapse and large voltages are created at the muzzle. If the voltage upon projectile exit is large enough, an arc will form at the armature contact surface and perhaps create an unpredictable pressure distribution on the projectile. This distribution can lead to launch problems.

DISTRIBUTION LIST

No. of Copies	Organization
12	Administrator Defense Technical Information Center ATTN: DTIC-DDA Cameron Station Alexandria, VA 22304-6145
1	HQDA (SARD-TR) Washington, DC 20310-0001
1	Commander US Army Materiel Command ATTN: AMCDRA-ST 5001 Eisenhower Avenue Alexandria, VA 22333-0001
1	Commander US Army Laboratory Command ATTN: AMSLC-DL Adelphi, MD 20783-1145
2	Commander Armament RD&E Center US Army AMCCOM ATTN: SMCAR-MSI Picatinny Arsenal, NJ 07806-5000
2	Commander Armament RD&E Center US Army AMCCOM ATTN: SMCAR-TDC Picatinny Arsenal, NJ 07806-5000
1	Director Benet Weapons Laboratory Armament RD&E Center US Army AMCCOM ATTN: SMCAR-LCB-TL Watervliet, NY 12189-4050
1	Commander Benet Weapons Laboratory Armament RD&E Center ATTN: SMCAR-CCB-RM Dr Patrick Votis Watervliet, NY 12189-4050
1	Commander Armament RD&E Center US Army AMCCOM ATTN: SMCAR-IMI-I Picatinny Arsenal, NJ 07806-5000
1	Commander Armament RD&E Center ATTN: SMCAR-CCJ Mr Joel Goldman Picatinny Arsenal, NJ 07806-5000
1	Commander Armament RD&E Center US Army AMCCOM ATTN: SMCAR-CCL-FA Mr Henry Kahn Picatinny Arsenal, NJ 07806-5000
2	Commander Armament RD&E Center US Army AMCCOM ATTN: SMCAR-CCL-F Mr Lucian Sadowski Mr Harry Moore Picatinny Arsenal, NJ 07806-5000
2	Commander Armament RD&E Center, CCAC ATTN: SMCAR-FSA-E Dr Thaddeus Gora Mr John Bennett Picatinny Arsenal, NJ 07806-5000

DISTRIBUTION LIST

No. of Copies	Organization
1	Commander US Army Armament, Munitions and Chemical Command ATTN: SMCAR-ESP-L Rock Island, IL 61299-5000
1	Commander US Army Aviation Systems Command ATTN: AMSAV-DACL 4300 Goodfellow Blvd St Louis, MO 63120-1798
1	Director US Army Aviation Research and Technology Activity Ames Research Center Moffett Field, CA 94035-1099
1	Commander US Army Missile Command ATTN: AMSMI-AS Redstone Arsenal, AL 35898-5010
1	Commander US Army Tank Automotive Command ATTN: ASQNC-TAC-DI (Technical Library) Warren, MI 48397-5000
1	Director U.S. Army TRADOC Analysis Command ATTN: ATAA-SL White Sands Misile Range, NM 88002-5502
1	Commandant U.S. Army Infantry School ATTN: ATSH-CD-CSO-OR Fort Benning, GA 31905-5660
1	AFWL/SUL Kirtland AFB, NM 87117-5800
1	Air Force Armament Laboratory ATTN: AFATL/DLODL Eglin AFB, FL 32542-5000
1	Air Force Armament Laboratory ATTN: AFATL/DLYS Lt. J Martin Mr. Kenneth Cobb Lt. D Jensen Eglin AFB, FL 32542-5000
1	Director Ballistic Missile Defense Advanced Technology Center ATTN: BMTADC-M Dr. Darrell B. Harmon P.O. Box 1500 Huntsville, AL 35898-5500

DISTRIBUTION LIST

No. of Copies	Organization
1	Commander Naval Surface Warfare Center ATTN: Mr. P. T. Adams G-35 Building Dahlgren, VA 22448
2	Commander Naval Research Laboratory ATTN: Mr. Ihor M. Vitkovitsky Code 4701. Mr Richard Ford Code 4774 Washington, DC 20375
1	AFAPL/POCS-2 ATTN: Dr. Charles Oberly Wright Patterson AFB Dayton, OH 45433
1	Director Brookhaven National Laboratory ATTN: J. R. Powell, Bldg 129 Upton, NY 11973
3	Director Los Alamos National Laboratory ATTN: MSG 787 Mr. Max Fowler Dr. Gerry V. Parker Dr. M. Parsons MS 1220 Los Alamos, NM 87545
1	NASA Lewis Research Center ATTN: Lynette Zana, MS 501-7 2100 Brook Park Rd. Cleveland, OH 44135
1	Director Defense Advanced Research Projects Agency ATTN: Dr Peter Kemmey 1400 Wilson Blvd. Arlington, VA 22209
1	Director Lawrence Livermore National Lab ATTN: Dr. R. S. Hawke, L-155 P.O. Box 808 Livermore, CA 94550
1	Commander Strategic Defense Initiative Org. ATTN: SDIO/KEW Maj. R. Lennard Washington, DC 20301-7100
3	Commander Strategic Defense Initiative Org. ATTN: SDIO/IST Dr. J. Ionson Dr. L. Caveny Washington, DC 20301-7100
1	Director Sandia National Laboratory ATTN: Dr. Maynard Cowan, Dept 1220 P.O. Box 5800 Albuquerque, NM 87185

DISTRIBUTION LIST

No. of Copies	Organization
1	University Of Tennessee Space Institute ATTN: Dr. Dennis Keefer Tullahoma, TN 37388-8897
4	University of Texas Center for Electromechanics Balcones Research Center ATTN: William Weldon Raymond Zaworka Dr. Dennis Peterson Mr. John Gully 10100 Burnett Rd. Bldg 133 Austin, TX 78758
1	University of Virginia Physics Dept ATTN: Doris Wilsdorf Jesse W. Beans Laboratory of Physics McCormick Rd. Charlottesville, VA 22901
1	Pacific-Sierra Research Corp. ATTN: Dr. Gene E. McClellan 1401 Wilson Blvd Arlington, VA 22209
1	General Defense Corp. ATTN: Mr. Hugh McElroy Flinchbaugh Division P.O. Box 127 Red Lion, PA 17356
2	Science Applications Inc. ATTN: Mr. Robert Acebal Dr. J. Batteh 1503 Johnson Ferry Rd. Suite 100 Marietta, GA 30062
1	Science Applications Inc. ATTN: Dr. Dan Barnes 206 Wild Basin Rd, Suite 103 Austin, TX 78746
1	Sparta, Inc. ATTN: Mr. Stuart Rosenwasser Mr. Dan Stevenson Mr. Dan Vrable 1104 B Camino Del Mar Del Mar, CA 92014
1	System Planning Corporation ATTN: Donald E. Shaw 1500 Wilson Blvd. Arlington VA 22209
2	Westinghouse Electric Corp. Marine Division ATTN: Dr. Dan Omry Dr. Ian R. McNab 401 E. Hendy Ave. Sunnyvale, CA 94088-3499
1	Westinghouse R&D Laboratory ATTN: Dr. Bruce Swanson 1310 Beulah Rd. Pittsburgh, PA 15233

DISTRIBUTION LIST

No. of Copies	Organization
1	Auburn University ATTN: Dr. R. F. Askew, Dir Leach Nuclear Science Center Auburn, AL 36849
1	Auburn University ATTN: Dr. E. J. Clothiaux Department of Physics Auburn, AL 36849
1	Texas University Dept of Electrical Engineering /Computer Science ATTN: Dr. M. Kristiansen Lubbock, TX 79409
1	Tuskegee Institute ATTN: Pradosh Ray Tuskegee, AL 35899
1	University of Miami ATTN: Dr. M. A. Huerta Physics Dept P.O. Box 248046 Coral Gables, FL 33124
1	Boeing Aerospace Compamy ATTN: Dr. J. E. Shraeder P.O. Box 3999 Seattle, WA 98134
3	Electromagnetic Research Inc. ATTN: Dr. Henry Kolm Dr. Peter Mongeau Dr. William Snow 625 Putnam Ave Cambridge, MA 62139
1	General Research Corp ATTN: Dr. William Isbell 5383 Hallister Ave Santa Barbara, CA 93111
1	GA Technologies ATTN: Dr. L. Holland P.O. Box 85608 San Diego, California 92138
1	GT Devices ATTN: Dr. Derek Tidman 5705-A General Washington Drive Alexandria, VA 22312
2	IAP Research ATTN: Dr. John Barber Dr. David P. Bauer 2763 Culver Ave. Dayton, OH 45429-3723
3	Maxwell Laboratories ATTN: Dr. Rolf Dethlefson Dr. Micheal Holland Dr. Mark Wilkinson 8888 Balboa Avenue San Diego, CA 92123
1	BDM ATTN: Jonathan Lee 950 Explorer Boulevard Huntsville, AL 35806

DISTRIBUTION LIST

No. of Copies | Organization

Aberdeen Proving Ground

Director, USAMSAA
ATTN: AMXSY-D
AMXSY-MP, Mr. H. Cohen

Commander, USATECOM
ATTN: AMSTE-TO-F

Cdr, CRDEC, AMCCOM
ATTN: SMCCR-RSP-A
SMCCR-SPS-IL
SMCCR-MU

USER EVALUATION SHEET/CHANGE OF ADDRESS

This laboratory undertakes a continuing effort to improve the quality of the reports it publishes. Your comments/answers below will aid us in our efforts.

1. Does this report satisfy a need? (Comment on purpose, related project, or other area of interest for which the report will be used.) _____

2. How, specifically, is the report being used? (Information source, design data, procedure, source of ideas, etc.) _____

3. Has the information in this report led to any quantitative savings as far as man-hours or dollars saved, operating costs avoided, or efficiencies achieved, etc? If so, please elaborate. _____

4. General Comments. What do you think should be changed to improve future reports? (Indicate changes to organization, technical content, format, etc.) _____

BRL Report Number _____ Division Symbol _____

Check here if desire to be removed from distribution list. ____

Check here for address change. ____

Current address: Organization _____
Address _____

----------FOLD AND TAPE CLOSED----------

Director
U.S. Army Ballistic Research Laboratory
ATTN: SLCBR-DD-T(NEI)
Aberdeen Proving Ground, MD 21005-5066

OFFICIAL BUSINESS
PENALTY FOR PRIVATE USE $300

BUSINESS REPLY LABEL
FIRST CLASS PERMIT NO. 12062 WASHINGTON D.C.
POSTAGE WILL BE PAID BY DEPARTMENT OF THE ARMY

NO POSTAGE NECESSARY IF MAILED IN THE UNITED STATES

Director
U.S. Army Ballistic Research Laboratory
ATTN: SLCBR-DD-T(NEI)
Aberdeen Proving Ground, MD 21005-9989